Structural Engineering and Mechanics, Vol. 5, No. 5 (1997) 541-552
DOI: http://dx.doi.org/10.12989/sem.1997.5.5.541

Nonlinear behavior of R/C cooling tower shells

Takashi Hara†

Department of Civil Engineering and Architecture,
Tokuyama College of Technology, Kume Takajo 3538, Tokuyama 745, Japan

Shiro Kato†

Department of Architecture and Civil Engineering,
Toyohashi University of Technology, Hibariga-oka 1-1, Toyohashi 441, Japan

Makoto Ohya‡

Department of Civil Engineering, Matsue National College of Technology,
Nishi-Ikuma 14-4, Matsue 690, Japan

Abstract. In this paper the ultimate strength of the R/C cooling towers, which have initial imperfection and pre-cracked elements, is analyzed. The initial geometric imperfections arise from the unavoidable inaccuracies under the construction and the pre-cracks are assumed to be produced by the temperature stress gradients or cyclic loading under wind pressure and/or earthquake load. Both effects are strongly influenced on the strength of the R/C cooling tower shell structures. The reinforcing ratio is also the important factor to evaluate the ultimate strength of the R/C cooling tower shells. However we could not analyze these structures experimentally because of their large geometry. Therefore, the numerical analyses are the powerful schemes to evaluate the safety and reliability of these structures. The analyzed model is Port Gibson cooling tower shell. In the numerical analysis the geometric and material nonlinearities are taken into account.

Key words: R/C shell; finite element analysis; ultimate strength; geometric imperfection; cooling tower

1. Introduction

Reinfored concrete (R/C) cooling towers are the huge structures ever constructed. These structures have an initial imperfection and a pre-cracked zone on the concrete surfaces. The initial geometric imperfections arise from the unavoidable inaccuracies under the construction and the pre-creaks are assumed to be produced by the temperature stress gradients or cyclic loading under wind pressure and/or earthquake load (Meshk, *et al.* 1991). Both effects strongly influence the strength of the R/C cooling tower shell structures. However we could not analyze these structures experimentally because of their large geometry. Therefore, the numerical analyses are

† Professor
‡ Assistant Professor

the powerful schemes to evaluate the safety and reliability of these structures. The numerical evaluations of the cooling tower strength have been done by many researchers. Mang, *et al.* (1983) analyzed the Port Gibson cooling tower by use of the nonliner finite element method and concluded that the strength of the R/C cooling tower was decided not by the instability problems but by the material nonlinear behavior. Milford (1984) analyzed the same structure focused on the tension stiffening of the concrete. Min, *et al.* (1992) analyzed the cooling tower shell by super computers. Hara, *et al.* (1994) also analyzed the Port Gibson cooling tower by use of the finite element method based on the isoparametric degenerate shell element.

In this paper the R/C cooling towers are analyzed by use of the finite element method. To evaluate the influences of the pre-cracking, we assume that the cracked concrete elements could not transfer the tensile stress arisen from the element deformation. The initial geometric imperfection considered in this analysis is the ring type and its amplitude varies in the inward direction. The ring type geometric imperfection plays an important role to the ultimate strength of the R/C hyperbolic cooling tower shell. From the numerical results the deformation properties and the crack distribution of the concrete surfaces are analyzed. Both the load increment scheme and the displacement increment scheme are adopted to avoid the instabilities of the solutions. The ultimate strength of the R/C cooling tower is detected from the load deflection behavior calculated in the analyses. The analyzed model is Port Gibson cooling tower shell. In the numerical analysis the geometric and material nonlinearities are taken into account.

2. Numerical procedure

The finite element method is adopted in the numerical analysis. In the nonlinear analysis of the R/C cooling tower, the following assumptions are used (Hara, *et al.* 1994). R/C hyperbolic cooling tower is discretized into the isoparametric degenerated shell elements. To avoid the numerical difficulties, Heterosis elements are adopted and the selective integration is used in the calculation. Considering the geometric nonlinear properties, the Green Lagrange nonlinear strain definitions are adopted. The layered approach is used to describe the material nonlinearities through the thickness.

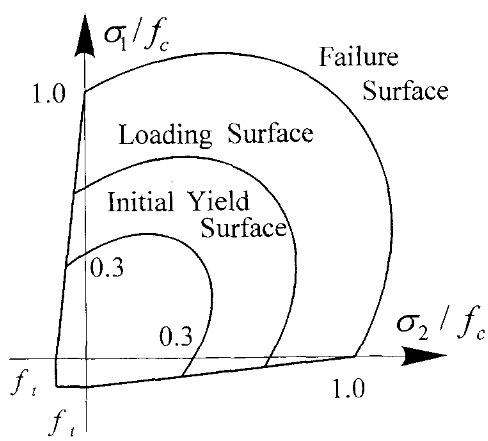

Fig. 1 Stress states in compressive concrete.

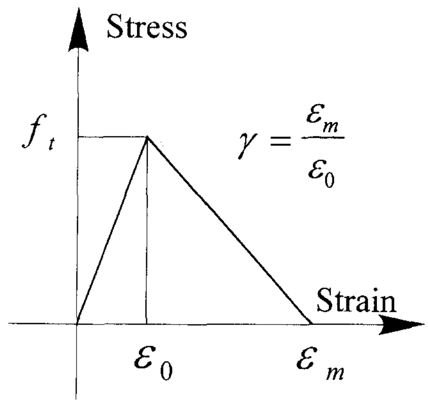

Fig. 2 Stress strain in tensile concrete.

To describe the material properties of the concrete and the reinforcements, some numerical assumptions are considered.

2.1. Material behavior of the concrete

The material properties of the concrete vary under the various stress condition. In the numerical analysis, following assumptions are adopted to present the concrete behavior.

2.1.1. Biaxial compression

The yield status of the concrete is defined by the Drucker Prager criterion, which is expressed as a following equation for the biaxial stress states (Fig. 1)

$$f(I_1, J_2) = \sqrt{\beta(3J_2) + \alpha I_1} = \sigma_0 \tag{1}$$

where I_1 and J_2 are the mean normal stress and the shear stress invariant, respectively. α and β are constants obtained from experimental results. In this paper, α and β are taken as 0.355 σ_0 and 1.355, respectively, based on the Kupfer's experiment (1969). σ_0 is the equivalent stress.

2.1.2. Elasto plastic-behavior

To represent the elasto-plastic behavior of concrete, the contributions of the elastic strain component and the inelastic strain component are separated. The elastic component behaves as the elastic material and the inelastic component behaves under the conventional flow rule. The strain hardening rule is defined by the Madrid Parabola.

2.1.3. Tensile concrete

For concrete in tension, tension stiffening (Fig. 2) is introduced (Hara, *et al.* 1994). In this model the concrete behaves as the linear elastic material up to the tensile strength and the stress degrades as shown in Fig. 2. The stress degradation rate is defined as the tension stiffening parameter γ (see Fig. 2).

$$\gamma = \frac{\varepsilon_m}{\varepsilon_0} \tag{2}$$

2.1.4. Crushing condition

It is assumed that the crushing is governed by the strain controlling phenomena. Therefore, the crushing condition is represented by the equation similar to Eq. (1), replacing the biaxial stress component by the biaxial strain component.

2.2. Material properties of reinforcement

The reinforcing steel is assumed to be the steel sheet that has a uniaxial bilinear constitutive relation and has the same properties both in compression and in tension.

2.3. Incremental scheme

To investigate the R/C cooling tower responses, both the load increment scheme and the displacement increment scheme are used for representing the nonlinear behavior and for avoiding the numerical instability caused by the sudden changes of the stress states due to the concrete cracks.

3. Numerical analysis

3.1. Numerical model

For the numerical model, the Port Gibson cooling tower (Grand Gulf power station, U.S.A.) is adopted. Fig. 3 shows the geometric dimension of the cooling tower. The configuration of the hyperbola is shown as follows:
Over the throat

$$-0.0026010z^3 - 0.038937rz + r^2 + 1.4174z - 36.7642r + 1278.6678 = 0 \tag{4}$$

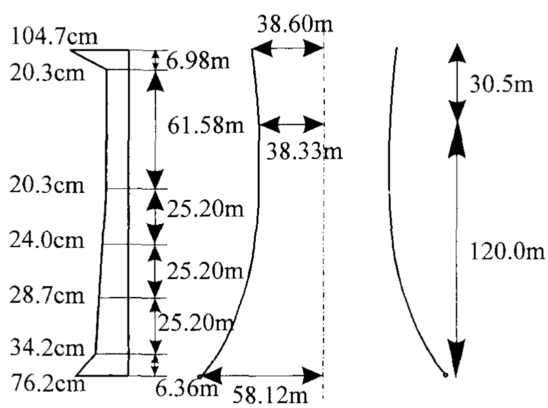

Fig. 3 Port Gibson cooling tower.

Table 1 Material properties

Concrete			Reinforcement		
Elastic modulus	E_c(MN/cm^2)	2.83	Elastic modulus	E_s (MN/cm^2)	20.59
Poisson's ratio	ν	0.18	Hardening modulus	E_t (MN/cm^2)	1.03
Density	ρ	2.43	Yield strength	σ_y (kN/cm^2)	41.37
Compressive strength	f_c (kN/cm^2)	3.45	Ultimate strength	σ_u (kN/cm^2)	62.05
Tensile strength	f_t (kN/cm^2)	0.32			

Table 2 Position of the reinforcement

Height z (m)	Thickness t (cm)	Position ζ
30.50	101.7	
23.52	20.3	0.820
−7.26	20.3	0.532
−22.65	20.3	0.532
−38.04	20.3	0.500
−63.24	24.0	0.529
−88.44	28.7	9.590
−113.64	34.2	0.678
−120.00	76.2	0.812

Table 3 Coefficient of the wind pressure

n	A_n	n	A_n	n	A_n	n	A_n
0	0.38330	1	−0.27918	2	−0.61978	3	−0.50927
4	−0.09167	5	0.11794	6	0.03333	7	−0.04474
8	−0.00833	9	−0.00972	10	−0.01356	11	−0.00597
12	−0.01667						

Below the throat

$$0.8602z^3 + 1.4208rz + r^2 - 51.7196z - 494.4638r + 16674.1904 = 0 \tag{5}$$

where z and the r denote the height measured from the throat and the radius of the shell in meters, respectively. The height and the shell thickness are about 150 m and 20 cm, respectively. The shell geometry is shown in the previous papert (Hare, *et al.* 1994). Table 1 shows the material properties of the cooling tower. The reinforcing ratio at the Port Gibson tower varies from 0.3% to 1.1% throughout the height and the reinforcing bars are doubly placed in both hoop and meridional dierction. The position of the reinforcement is shown in Table 2. In the numerical analysis we assume the constant reinforcing ratio throughout the height to clarify the influence of the reinforcing raion on the ultimate strength of the cooling tower. However, the shell configuration is modeled based on the actual cooling tower.

3.2. Load

The wind pressure adopted in this analysis is the same distribution pattern as Mang, *et al.* (1983) and Hara, *et al.* (1994). The distribution in hoop direction is as follows:

$$H_\alpha = -0.5 + \sum_{n=0}^{12} A_n \cos n\theta \tag{6}$$

where A_n is the amplitude shown in Table 3. The distribution of the wind pressure through the meridional direction $p[N/m^2]$ is as follows:

$$p = 413.013 H_\alpha (3.281z + 393.696)^{2/7} \tag{7}$$

where $z[m]$ is the distance from the throat. The maximum compressive wind pressure is denoted around the region of about 80 degree from the windward in the hoop direction. In the numerical analysis, the self weight is applied to the cooling tower model gradually. After the loading level reaches to the self weight, the wind pressure defined in Eq. (7) is applied quasi statically.

3.3. FE model

The numerical model is the Port Gibson cooling tower. The model is an exact half of the tower considering the symmetry of the loading and supporting condition and is simply supported at the bottom and free at the top. The shell is divided into the 12 elements in meridional direction and the 8 elements in hoop direction (see Fig. 4). Each shell element is composed of the 8 concrete layers and the 4 steel layers to evaluate the stress distribution through the

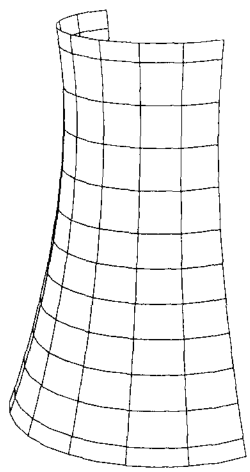

Fig. 4 Finite element mesh.

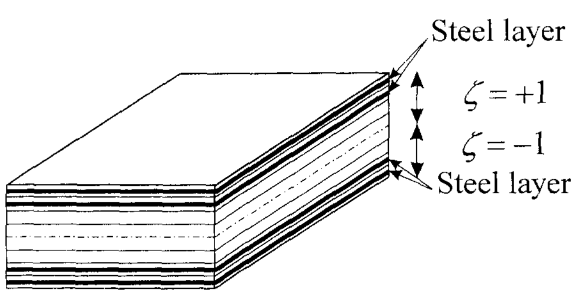

Fig. 5 Layer pattern.

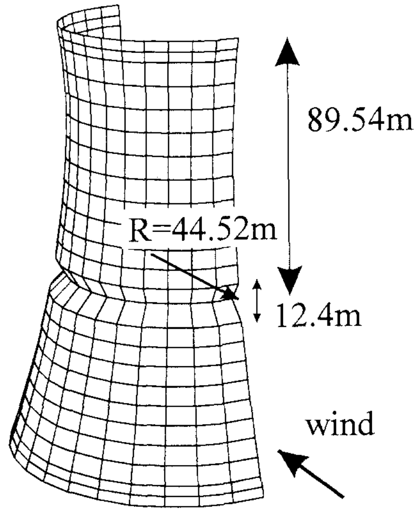

Fig. 6 Geometric imperfection.

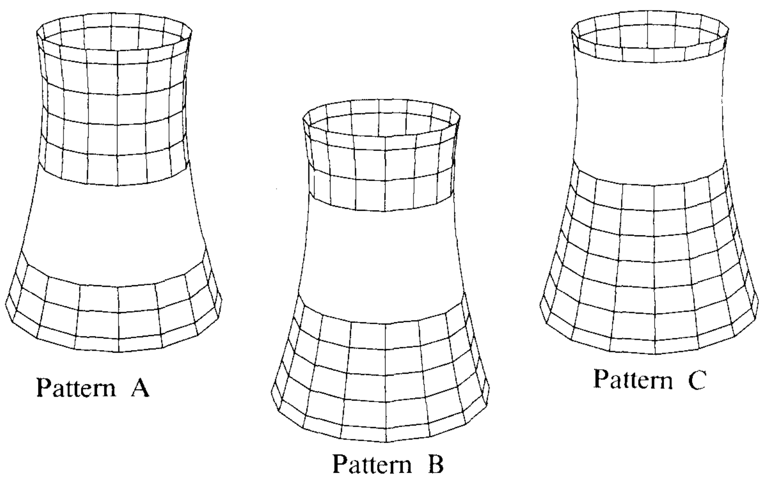

Fig. 7 Pre-crack pattern.

thickness. The typical layer pattern is shown in Fig. 5. The elements are derived on the basis of the isoparametric degenerated shell element.

In the numerical analysis, we assumed that the cooling tower has the ring type of initial geometric imperfection caused by the inavoidable constructional inaccuracy (Fig. 6). The position of the ring imperfection is defined by the condition that the maximum compressive strength occurs on that position under the wind pressure. The various imperfection amplitude is adopted as the numerical parameter. Also three types of pre-cracked patterns are adopted (Fig. 7). Pattern A and Pattern B are defined by possessing the pre-cracked zone around the lower portion and the middle portion of the cooling tower, respectively. Pattern C means that the cooling tower possesses the pre-cracked zone around the upper portion of the cooling tower. The reinforcing ratio is also adopted as the numerical parameter.

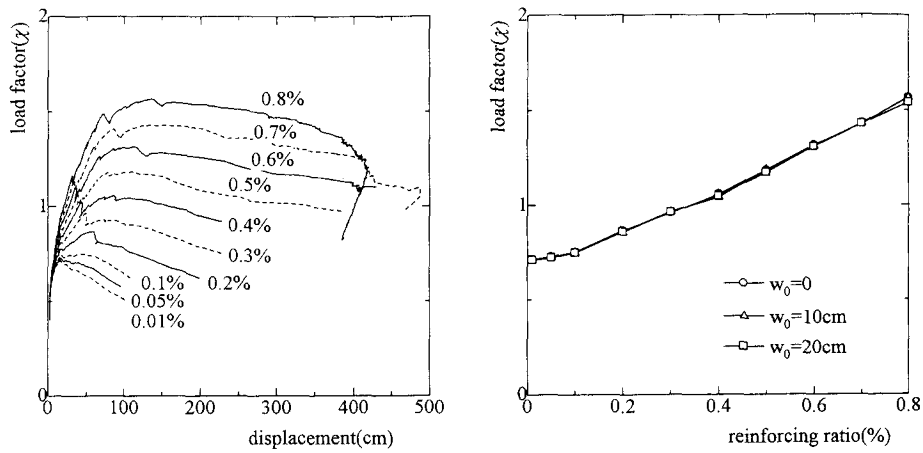

(a) Influence of reinforcement ($w_0=0$)
(b) Influence of reinforcement and geometric imperfection

Fig. 8 Load deflection behavior (Pattern A).

4. Numerical results

The gravity load is applied gradually by the load incremental scheme. Then the wind pressure is applied by the displacement increment scheme to aviod the numerical instability caused by the concrete failure and the concrete deterioration. The load factor χ defined by the following equation.

$$U = 1.0D + \chi p \tag{8}$$

where U, D and p are the total loading, the self weight and the wind pressure defined by Eq. (7), respectively. In the numerical analysis, the displacement is measured at the throat on the windward meridian.

4.1. Load deflection behavior of the cooling tower with pre-crack pattern A

Fig. 8 shows the load deflection behavior of the cooling tower under the various reinforcing ratio and the initial geometric imperfection. The cooling tower has the pre-crack pattern of type A. Fig. 8(a) shows the load deflection curve of the cooling tower. The displacement grows up before initial cracks. Then the load factor decreases with the reduction of the stiffness. The load-displacement curves decrease with the large displacement after detecting the ultimate strength. The larger the reinforcement is the larger the ultimate strength of the cooling tower. Fig. 8(b) shows the influence of the geometric imperfection on the ultimate strength. The ultimate strength is defined as the maximum load factor denoted in Fig. 8(a). Fig. 8(b) shows that the geometric imperfection defined in this paper does not influence on the ultimate strength.

4.2. Load deflection behavior of the cooling tower with pre-crack pattern B

Fig. 9(a) shows the load deflection behavior of the cooling tower shell with pre-crack pattern B. The shell shows larger stiffness than that of pattern A. However, the reduction of the stiffness

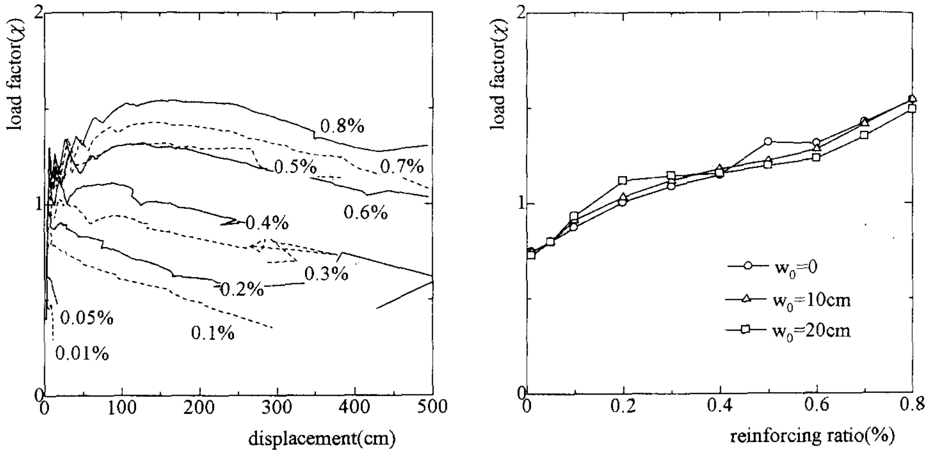

(a) Influence of reinforcement ($w_0=0$) (b) Influence of reinforcement and geometric imperfection

Fig. 9 Load deflection behavior (Pattern B).

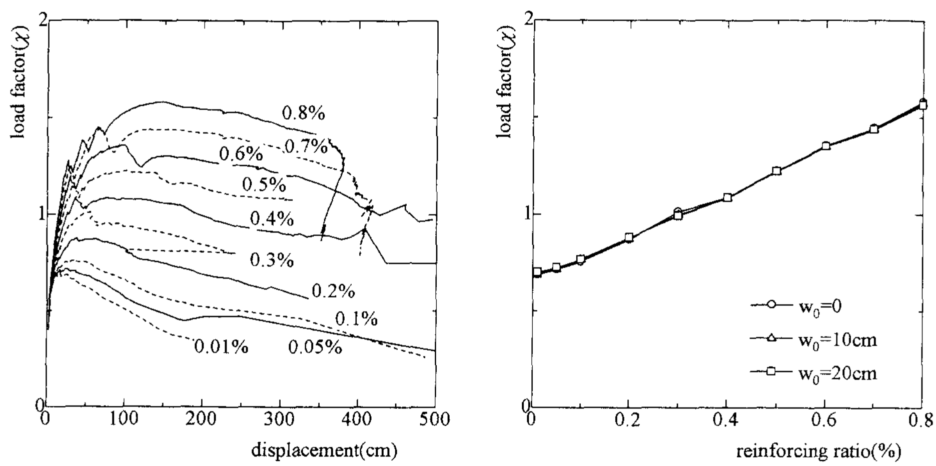

(a) Influence of reinforcement ($w_0=0$) (b) Influence of reinforcement and geometric imperfection

Fig. 10 Load deflection behavior (Pattern C).

after cracks is steeper than that of pattern A, especially in the lower reinforcing ratio. The relation between the strength and the reinforcement shows the same tendencies as Fig. 8. Fig. 8(b) shows the influence of the initial imperfection on the ultimate strength of the cooling tower. The ultimate strength shows the irregular form because the load deflection curves strongly depend on the reinforcing ratio (see Fig. 8(a)). Especially, the ultimate strength is strongly influenced by the reinforcing ratio. Therefore, the shell with pre-crack pattern B is influenced both by the reinforcement and by the initial geometric imperfection. The influences on the ultimate strength are within 10% through 15%.

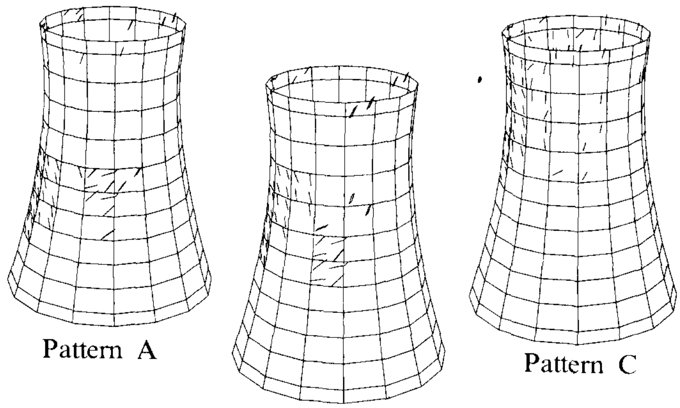

Fig. 11 Final crack pattern.

4.3. Load deflection behavior of the cooling tower with pre-crack pattern C

Fig. 10 shows the load deflection behavior of the cooling tower shell with pre-cracked pattern C. The load deflection behavior denoted in Fig. 10(a) shows the same tendencies as Fig. 8(a). Also, the ultimate strength of the cooling tower is not influenced by the initial geometric imperfection.

4.4. Final crack pattern

Fig. 11 shows the final crack pattern on the outer surface of the cooling tower with reinforcing ratio of 0.4% and without initial geometric imperfection. Cracks are spread within the upper ring in addition to the pre-cracked region. The cracks around the middle or the lower part of the cooling tower strongly influence on the ultimate strength (Hara, *et al.* 1994).

4.5. Relation between the ultimate strength and the design recommendation

Fig. 12 shows the ultimate strength with various pre-cracked pattern. Here the initial geometric imperfection is not taken into account. The abscissa and the ordinate show the reinforcing ratio and the ultimate strength. Vertical lines denoted in the figure show the IASS and ASCE-ACI reinforcing requirement, respectively. IASS and ASCE-ACI recommend the appropriate reinforcing ratio for the complete cooling tower shells. However, the ultimate strength of the cooling tower with pre-cracked pattern shows the lower strength than the designed strength which is shown as the horizontal solid line. Also the ultimate strength shows the lower strength than the recommended ultimate strength which is shown by the horizontal dotted line. In the case of large reinforcement, the numerical results show almost the same ultimate strength. Therefore, the more reinforcements are needed considering the deterioration of the cooling tower stiffness due to the concrete ageing effects and the reinforcement corrosion.

5. Conclusions

To investigate the influences of the initial geometric imperfection and the ageing effect on

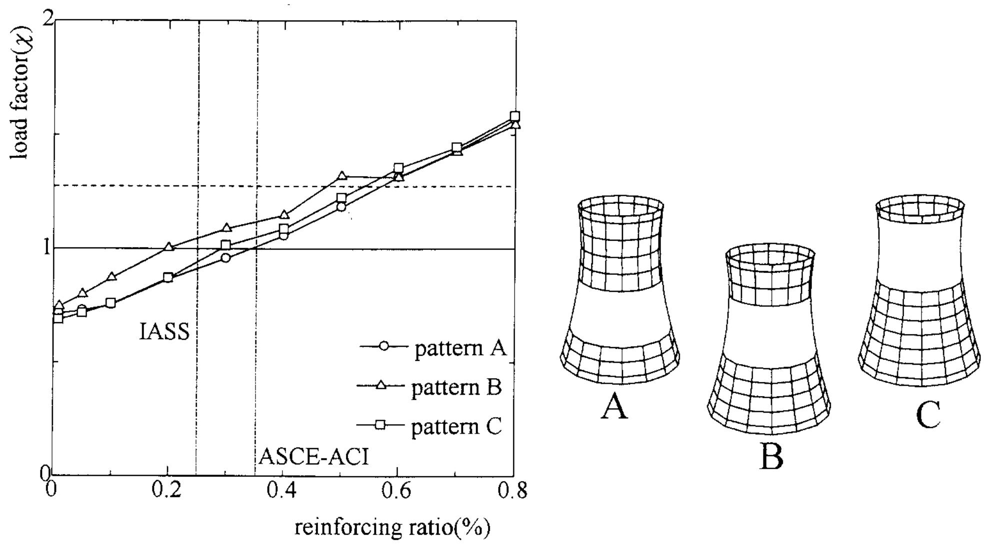

Fig. 12 Influence of reinforcement and geometric imperfection.

the ultimate strength of the R/C cooling tower, both the load deformation behavior and the ultimate strength is analyzed of use by the finite element method. From the numerical analyses following conclusions are obtained.

1. The influences of the initial geometric imperfection on the ultimate strength of the cooling tower are not so large except the pre-cracking of pattern B.

2. From the load-deflection curves of pattern B, the model with this crack pattern has larger stiffness than other crack pattern. Pattern A and pattern C have almost the same behavior and both response are smaller stiffness than pattern B. Therefore, the lower and the upper cracking zone show the strong influences on the strength of the cooling tower shell.

3. The cooling tower with large amount of reinforcement shows the large ultimate strength without concerning the pre-cracked pattern.

4. IASS and ASCE-ACI recommend the appropriate reinforcing ratio. However, more reinforcements are needed considering the deterioration of the cooling tower stiffness due to the concrete ageing effects and the reinforcement corrosion.

References

ACI-ASCE Committee 334 (1984), "Reinforced concrete cooling tower shell - practice and commentary", *ACI Journal*, **81**, 623-631.

Hara, T., Kato, S. and Nakamura, H. (1994), "Ultimate strength of RC cooling tower shells subjected to wind load", *Engineering Structures* **16**(3), 171-180.

Hinton, E. and Owen, D.J.R. (1984), *Finite Element Software for Plates and Shells*, Press, Swansea, UK.

IASS Working Group 3 (1977), *Recommendation for the Design of Hyperbolic or Other Similarly Shaped Cooling Towers*. BRUSSELS.

IASS The Working group on recommendations of IASS (1979), *Recommendations for Reinforced Concrete Shell and Folded Plates*. MADRID.

Krätzig, W.B. Gruber, K. and Zahlten, W. (1992), *Numerical Collapse Simulation of Large Cooling Towers Checking Their Safety and Durability*, Technical Reports Ruhr-Universitat Bochum No. 92-3.

Kupfer, H. and Hilsdorf, K.H. (1969), "Behavior of concrete under biaxial stress", *ACI Journal* **66**(8), 656-666.
Mang, H.A. and Floegl, H. (1983), "Wing-load reinforced concrete cooling towers: buckling or ultimate load?", *Engineering Structures*, **5**(7), 163-180.
Meshk, M, Mang, H.A. and Kosza, P. (1991), "Finite element analysis of cracked cooling tower shell" *Journal of Structural Engineering* **117**(9), 2620-2635.
Milford, R.V. (1984), "Nonlinear behavior of reinforced concrete cooling towers", PhD thesis, University of Illinois at Urbana.
Min, C.S. and Gupta, A.K. (1992), "A study of inelastic behavior of reinforced concrete shells using supercomputers", *Reinforced Concreted Shell Research Report*, North Carolina State University.